

Article

Potential Suitable Habitat of Two Economically Important Forest Trees (*Acer truncatum* and *Xanthoceras sorbifolium*) in East Asia under Current and Future Climate Scenarios

Yaoping Wu^{1,2}, Yong Yang², Cheng Liu^{2,3}, Yixuan Hou^{1,2}, Suzhi Yang⁴, Liangsheng Wang^{2,3} and Xiuqing Zhang^{1,*}

- ¹ Forest College, Inner Mongolia Agricultural University, Hohhot 010019, China; arcsin180@126.com (Y.W.); h_yxuan@126.com (Y.H.)
- ² Key Laboratory of Plant Resources, Beijing Botanical Garden, Institute of Botany, Chinese Academy of Sciences, Beijing 100093, China; yangyong20092515@163.com (Y.Y.); liucheng@ibcas.ac.cn (C.L.); wanglsh@ibcas.ac.cn (L.W.)
- ³ University of Chinese Academy of Sciences, Beijing 100049, China
- ⁴ Science and Technology Section, Chifeng Research Institute of Forestry Science, Chifeng 024005, China; yangsuzhi_999@163.com
- * Correspondence: 18686081487@163.com; Tel.: +86-18686081487

Abstract: *Acer truncatum* Bunge and *Xanthoceras sorbifolium* Bunge are small deciduous trees distributed in East Asia and have high ecological and nutrient value due to their strong environmental adaptability and seed oil abundant in nervonic acid and unsaturated fatty acids. However, their natural distribution remains unclear, which will also be affected by the changing climatic conditions. The main purpose of this study was to map and predict the current and future potential suitable habitats of these two species using MaxEnt based on the presence location of species and environmental variables. The results showed that *A. truncatum* was more suitable for warm and humid climates and was more durable to climate change compared to *X. sorbifolium*. Under the current environmental conditions, the suitable habitat of *A. truncatum* was mainly concentrated in Inner Mongolia Plateau, Loess Plateau, Sichuan Basin, Northeast Plain, North China Plain, Korean Peninsula, as well as Japan, with an area of $115.39 \times 10^4 \text{ km}^2$. *X. sorbifolium* was mainly distributed in Inner Mongolia Plateau and Loess Plateau with an area of $146.15 \times 10^4 \text{ km}^2$. Under future climate scenarios, the model predicted that higher concentrations of greenhouse gas emissions could result in greater expansion of the potential distribution of both species. Meanwhile, the study also revealed that the two species migrated to the north by east to varying degrees with the change in suitable habitats. This work could provide scientific basis for resource protection and utilization of the two economic forest trees.

Keywords: climate change; woody oil crops; MaxEnt; potential distribution; environmental variables



Citation: Wu, Y.; Yang, Y.; Liu, C.; Hou, Y.; Yang, S.; Wang, L.; Zhang, X. Potential Suitable Habitat of Two Economically Important Forest Trees (*Acer truncatum* and *Xanthoceras sorbifolium*) in East Asia under Current and Future Climate Scenarios. *Forests* **2021**, *12*, 1263. <https://doi.org/10.3390/f12091263>

Academic Editor: Didzis Elferts

Received: 27 August 2021

Accepted: 13 September 2021

Published: 16 September 2021

Publisher's Note: MDPI stays neutral with regard to jurisdictional claims in published maps and institutional affiliations.



Copyright: © 2021 by the authors. Licensee MDPI, Basel, Switzerland. This article is an open access article distributed under the terms and conditions of the Creative Commons Attribution (CC BY) license (<https://creativecommons.org/licenses/by/4.0/>).

1. Introduction

The temporal and spatial variation of climate has a direct and profound influence on the distribution pattern of species, especially on the growth and population size of plants [1–3]. However, changes in surface vegetation also directly affect global climate change. [4–6]. The Intergovernmental Panel on Climate Change (IPCC) Sixth Assessment Report revealed that the global average surface temperature in the last 10 years (2011–2020) was 1.09 °C higher than that in 1850–1900, and 0.19 °C warmer than that in 2003–2012 (the period assessed in the fifth Assessment report). These data indicate that global temperature is still rising, and global warming has not stopped (IPCC, 2021) [7]. In addition, the global precipitation pattern is also changing, with arid areas becoming drier and humid areas becoming wetter [8,9]. These environmental changes will unquestionably affect the distribution of plant species.

The wild distribution of *Acer truncatum* is mainly located in North China Plain and Korean Peninsula, and the wild distribution of *Xanthoceras sorbifolium* is mainly located in the Loess Plateau and Inner Mongolia Plateau. *A. truncatum* and *X. sorbifolium* are two high-yield and high-quality woody oil crops with huge development potential. Both are deciduous broadleaf trees, which are widely cultivated in China due to their important economic value. The seed kernels of *A. truncatum* and *X. sorbifolium* are rich in fatty acids, especially unsaturated fatty acids, such as oleic acid (OA) and linoleic acid (LA) [10,11]. OA is a monounsaturated fatty acid with only one carbon–carbon double bond in the carbon chain [12], which has physiological effects, such as regulating blood lipids and reducing cholesterol. LA is an unsaturated fatty acid with two carbon–carbon double bonds in the carbon chain. As an essential fatty acid, it cannot be synthesized in the human body and must be taken from food. LA plays an important role in regulating body function [13,14]. Moreover, the seed oil of *A. truncatum* and *X. sorbifolium* contains more than 5 and 3% of nervonic acid (NA), respectively, which are generally absent in other vegetable oils. NA are essential nutrients for brain development and maintenance and can prevent diseases, such as Alzheimer’s disease, brain atrophy, and memory decline. It can also be added to infant formula food as a food additive to promote infant intellectual development and improve memory. It is mainly used in health products and drugs [15,16]. In fact, NA is most abundant in the seed kernel of *Malania oleifera* Chun & S.K.Lee (>60%). However, *M. oleifera* is an IUCN red listed tree and restricted to the Karst region of southwest China [17]. *A. truncatum* and *X. sorbifolium*, with much broader distribution, large fruits and considerable yield of nervonic acid are promising new resources for NA. In addition, *A. truncatum* and *X. sorbifolium* have strong environmental adaptability and beautiful tree shape; therefore, they are often used for street trees and desertification control. At present, *A. truncatum* has been widely planted as afforestation tree species in China, Korea and Japan [18,19], and *X. sorbifolium* has large-scale cultivation in Northwest, Central and North China [20].

Predicting plant distribution through models under future climate change is the basis for increasing economic productivity and reducing ecosystem damage [21]. Species distribution models (SDMs) combine the environmental variables with the actual species distribution points to simulate the changes of ecological niche in time and space [22]. Researchers have developed a variety of SDMs models such as bioclimatic modeling [23], genetic algorithm of rule set production [24], domain environmental envelope [25], and maximum entropy (MaxEnt) [26] according to their needs. Among them, the MaxEnt model has good explanatory power for the adaptability of species habitat in various research [15,27,28]. In recent years, MaxEnt has been used to simulate the potential suitable habitat of various organisms, and good prediction results have been achieved [29,30].

With global climate change, the research on the potential geographical distribution of *A. truncatum* and *X. sorbifolium* in the future will provide theoretical support for the development and reasonable promotion of these two economic forest trees [31]. In this study, a MaxEnt model was used to predict the potential distribution of *A. truncatum* and *X. sorbifolium*. Under the current and future climate scenarios, the centroid positions and migration trend of the two species were simulated, and their suitable habitats were quantified. This study will facilitate rational development and utilization of these two species and the construction of ecological industry in the case of climate change in the future.

2. Materials and Methods

2.1. Species Occurrence Data

Species occurrence data of *A. truncatum* and *X. sorbifolium* were obtained from the Global Biodiversity Information Facility (GBIF, <https://www.gbif.org/>, accessed on 8 June 2021), the Chinese Virtual Herbarium (CVH, <http://www.cvh.ac.cn/>, accessed on 8 June 2021), and field surveys. In order to ensure the accuracy of the data, the collected occurrence records were screened as follows: (1) repeated occurrence records were removed and each occurrence records had accurate geographical coordinates. (2) With the help of ArcGIS (version 10.5, ESRI, Redlands, CA, USA), the records were spatially filtered so that only

one record appeared in each grid (10×10 km) cell to correct the sampling bias. (3) The occurrence records under different environmental variables were stratified and sampled by ArcGIS, and then the corresponding environmental data of all distribution points were derived and screened to ensure that each record had accurate corresponding environmental variable values. The above operations could correct the sampling deviation and ensure the accuracy of occurrence records in niche model construction. Finally, 242 occurrence records of *A. truncatum* and 102 occurrence records of *X. sorbifolium* were obtained (Figure 1).

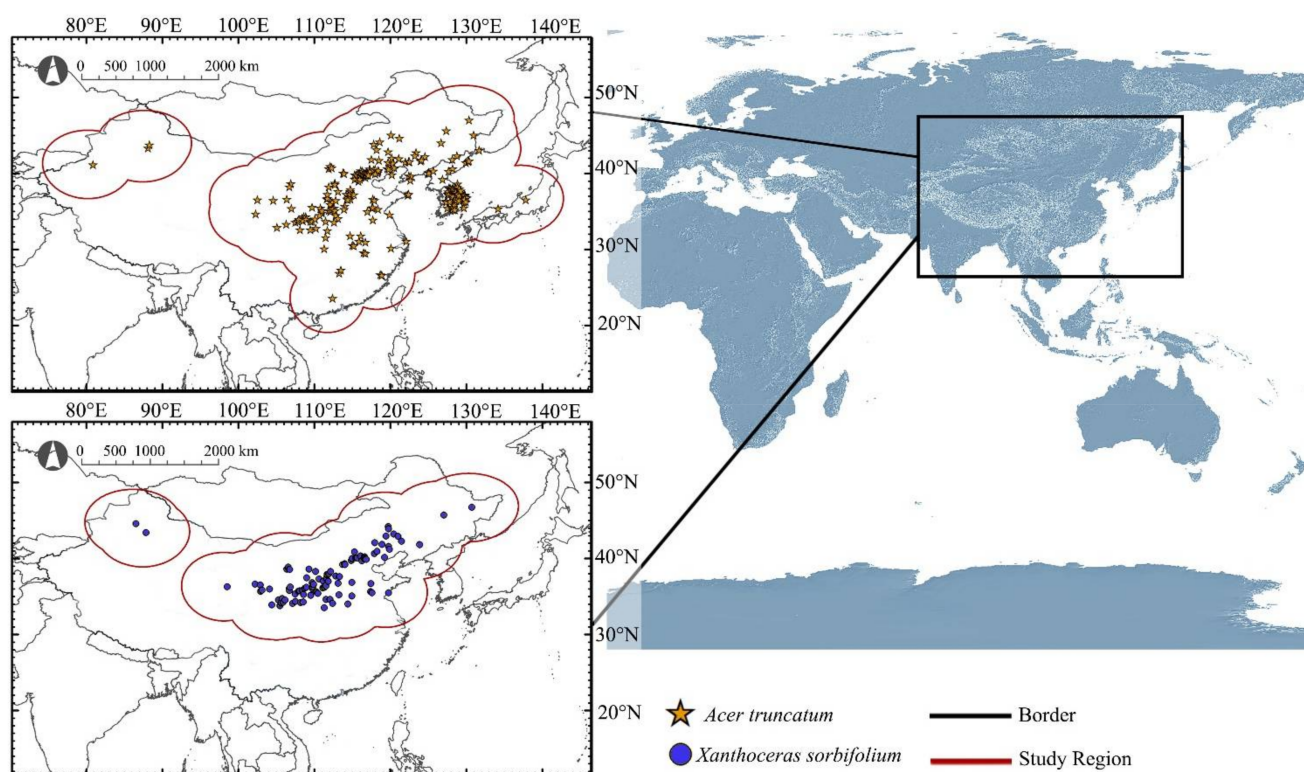


Figure 1. Distribution records and study regions of *A. truncatum* and *X. sorbifolium*.

2.2. Study Regions

In this study, areas of 500 km radius outside all the occurrence records of *A. truncatum* and *X. sorbifolium*, respectively, were set as buffers. Then, all the buffers were superimposed to form a buffer of study region for each species (Figure 1). The two study regions formed included all possible migration events under future climatic conditions and reduced extrapolations when projecting under other or larger dominant climate conditions. These two species are widely distributed in the natural environment and cross geographic barriers such as mountains and oceans in the study area, so geographic factors can be ignored. At the same time, study regions also contained the candidate areas that species may reach in the future as a result of assisted migration [27].

2.3. Environmental Variables

In this study, 31 environmental variables that may affect *A. truncatum* and *X. sorbifolium*, respectively, were selected to predict current and future habitats of the two tree species. Among them, 19 bioclimatic variables came from the World Climate Database (<https://www.worldclim.org>, accessed on 8 June 2021) [32]. Growing degree day (GDD), soil pH (SpH), and soil organic carbon (SC) were derived from global sustainable development (<https://nelson.wisc.edu/sage/>, accessed on 8 June 2021) [33]. Ground-frost frequency (FRS), wet-day frequency (WET) and vapor pressure (VAP) were derived from IPCC (<https://www.ipcc.ch/data/>, accessed on 8 June 2021), and global ultravi-

olet UVB1–6 were derived from gIUV database (<https://www.ufz.de/gIUV/>, accessed on 8 June 2021) [34].

Future bioclimatic variables were derived from CCSM4 (Community Climate System Model v. 4.0), developed by the Center for Atmospheric Research (Boulder, CO, USA). Four emission scenarios of RCP (representative concentration pathways) 2.6, RCP4.5, RCP6, and RCP8.5, which represent all possible ranges of total radiative forcing values +2.6, +4.5, +6.0, and +8.5 W/m² in 2100 relative to those before industrialization, were established in the fifth IPCC climate assessment report [35]. In this study, four climate scenarios of 2050s and 2070s were used to simulate and predict the future suitable habitats. The changes in these habitats over time could be observed through comparing. The remaining environmental factors (GDD, SpH, SC, FRS, WET, VAP, and UVB1-6) were fixed in the prediction of potential distribution areas in the future.

All the environmental variables were resampled. The unified spatial resolution was 30" (approximately 0.86 km²). In order to avoid the interferences between the selected environmental factors, the variance inflation factor (VIF) was used to eliminate the data with high correlation coefficient. First, 10,000 random distribution points were created in the study regions of *A. truncatum* and *X. sorbifolium*, respectively. The data of the 31 environmental factors of each distribution point were sampled and screened, which would be retained with VIF value less than 10 [36].

In the MaxEnt, a jackknife test is used to calculate the contribution rate of environmental variables to species distribution, which is used to determine the main environmental variables affecting species distribution.

2.4. Assessment of Current and Future Habitats

The occurrence records of *A. truncatum* and *X. sorbifolium*, respectively, and the environmental variables at different periods were imported into MaxEnt 3.4.3 (http://biodiversityinformatics.amnh.org/open_source/maxent/, accessed on 8 June 2021) for the simulation of suitable habitats. Additionally, 75% of the distribution point data were randomly screened as the training set, and the remaining 25% of the samples were used to verify the model. The simulation calculation was repeated 20× in the way of secondary sampling, and the maximum number of iterations was 1000. The accuracy of the simulation results was tested by drawing the receiver operating characteristic (ROC) curve; the area under curve (AUC) of the ROC curve reflected the accuracy of the simulation results [37]. AUC was used to evaluate model performance, with 0.7 < AUC < 0.8, 0.8 < AUC < 0.9, and AUC > 0.9 indicating acceptable, good, and highly accurate model performance, respectively [38,39].

The predicted results of the MaxEnt model, ranging from 0 to 1, showed the survival probability of species in the region. The reclassification of ArcGIS10.5 software was used for classification, and the results categorized into four degrees, including no suitability (0–0.2), low suitability (0.2–0.4), moderate suitability (0.4–0.6), and high suitability (0.6–1), based on the predicted probability of presence [40].

The shape of the potential suitable habitat is irregular, so the center point of the potential distribution is defined by the Centroid to characterize the migration of the location of the species suitable habitat under current and future climate change scenarios. The habitat distributions of *A. truncatum* and *X. sorbifolium* were, respectively, transformed into binary images using SDM tools (a type of python-based ArcGIS software) with a threshold of 0.6. Then, the centroid position of each species in the current and future habitats were calculated. The migration and centroid changes of the two species under different climate scenarios were compared [41].

3. Results

3.1. Accuracy Test

Based on the species occurrence records and related biological environmental variables of *A. truncatum* and *X. sorbifolium*, respectively, the AUC values of *A. truncatum* and

X. sorbifolium were 0.862 and 0.890, respectively, indicating that the prediction results were accurate.

3.2. Important Environmental Variables

According to VIF, 13 environment variables of *A. truncatum* and *X. sorbifolium* were established as the evaluation factors (Table 1).

Table 1. Percentage contributions and permutation importance of the environmental variables in the Maxent models of *A. truncatum* and *X. sorbifolium*. Variables without any values (indicated by ×) were removed due to high cross-correlations.

Symbol	Bioclimatic Variables	<i>A. truncatum</i>		<i>X. sorbifolium</i>	
		Contribution (%)	Permutation Importance (%)	Contribution (%)	Permutation Importance (%)
BIO2	Mean Diurnal Range	0.4	0.3	3.1	1.3
BIO8	Mean Temperature of Wettest Quarter	0.4	0.5	2.3	11.2
BIO9	Mean Temperature of Driest Quarter	41.5	30.7	33.8	27.5
BIO13	Precipitation of Wettest Month	31.2	29.9	23.8	23.8
BIO14	Precipitation of Driest Month	×	×	16	14.1
BIO15	Precipitation Seasonality (Coefficient of Variation)	8.7	2.4	2.7	4.5
BIO19	Precipitation of Coldest Quarter	1.4	1.4	×	×
GDD	Growing Degree Days	2.9	6	5.2	6.1
SC	Soil Organic Carbon	1.2	0.5	3.7	5.3
SpH	Soil pH	2.1	2.9	4.5	1.1
VAP	Vapor Pressure	1.2	3.3	1.3	2.3
WET	Wet-Day Frequency	1	11	1.8	2.3
UVB-2	UV-B Seasonality	8	11	1.8	0.4

The main environmental variables affecting the distribution of *A. truncatum* were mean temperature of driest quarter (Bio9, 41.5% of variation), precipitation of wettest month (Bio13, 31.2% of variation), precipitation seasonality (Bio15, 8.7% of variation), and UV-B seasonality (UVB-2, 8% of variation), with a cumulative contribution rate of 89.4% (Table 1). The main environmental factors affecting *X. truncatum* distribution were mean temperature of driest quarter (Bio9, 33.8% of variation), precipitation of wettest month (Bio13, 23.8% of variation), and precipitation of driest month (Bio14, 16% of variation); the cumulative contribution rate of the above environmental variables was 73.6% (Table 1).

The variation range of the main environmental variables restricting the growth of *A. truncatum* was as follows: the temperature in the driest season was -10 to 4 °C, the precipitation in the wettest month was 110 to 680 mm, the precipitation seasonality was >65 , and the seasonal variation of UV was 120,000 to 155,000 $\text{JM}^{-2}\cdot\text{d}^{-1}$. The variation range of the main environmental factors restricting the growth of *X. sorbifolium* was as follows: the temperature in the driest season was -10 to 1 °C, the precipitation in the wettest month was 60 to 150 mm, and the precipitation in the driest month was 1 to 9 mm (Figure 2).

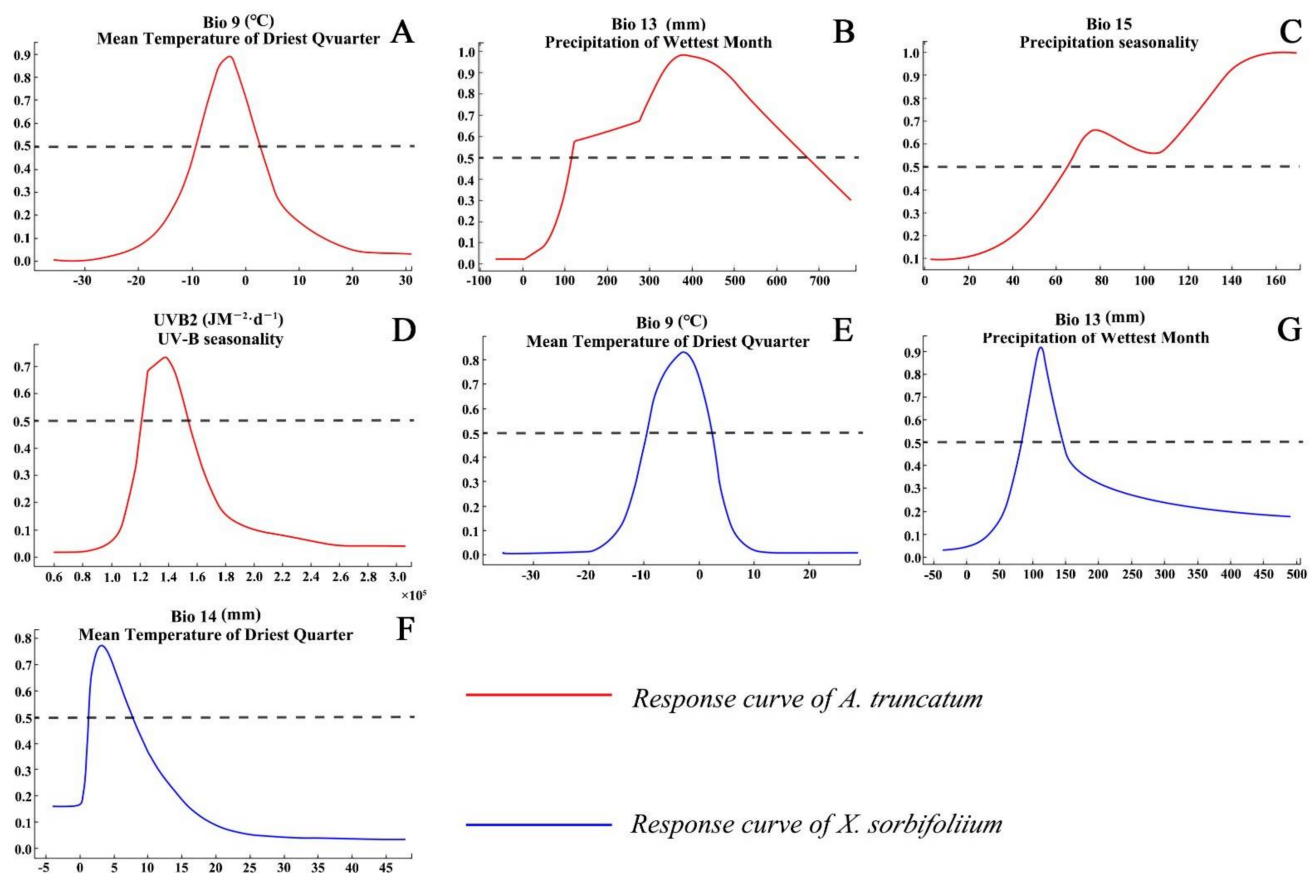


Figure 2. Response curves of the major environmental variables important for *A. truncatum* (A–D) and *X. sorbifolium* (E,F).

3.3. Current Potential Suitable Habitats

Under current climate conditions, the MaxEnt model projected that *A. truncatum* was mainly distributed in 28° N–46° N, 102° E–143° E. The potential habitats of high suitability, medium suitability, and low suitability were 53.19×10^4 km², 25.55×10^4 km², and 36.65×10^4 km², respectively (Table 2). The potential suitable habitats of *A. truncatum* were mainly in Inner Mongolia Plateau, Loess Plateau, Sichuan Basin, Northeast Plain, North China Plain, Korean Peninsula, and Japan, with an area of 115.39×10^4 km² (Figure 3).

Table 2. Potential suitable areas of different grades of *A. truncatum* and *X. sorbifolium* under current and future four climate scenarios (2050s and 2070s).

	<i>A. truncatum</i> ($\times 10^4$ km ²)				<i>X. sorbifolium</i> ($\times 10^4$ km ²)			
	High	Moderate	Low	Total	High	Moderate	Low	Total
Current	53.19	25.55	36.65	115.39	37.23	24.29	35.47	97
RCP2.6—2050	65.89	43.23	47.96	157.08	44.37	28.94	60	133.31
RCP2.6—2070	61.08	36.06	40.75	137.9	37.99	28.48	60.49	126.96
RCP4.5—2050	66.17	41.32	46.64	154.12	48.55	31.38	66.36	146.29
RCP4.5—2070	67.3	45.94	53.37	166.61	45.29	31.79	74.67	151.75
RCP6.0—2050	65.9	36.82	45.54	148.26	44.28	28.42	64.86	137.56
RCP6.0—2070	62.75	45.23	51.43	159.4	47.11	33.29	78.03	158.43
RCP8.5—2050	72.4	42.45	52.94	167.79	48.61	34.97	77.22	160.8
RCP8.5—2070	61.63	62.59	71.19	195.42	58.37	32.34	102.19	192.9

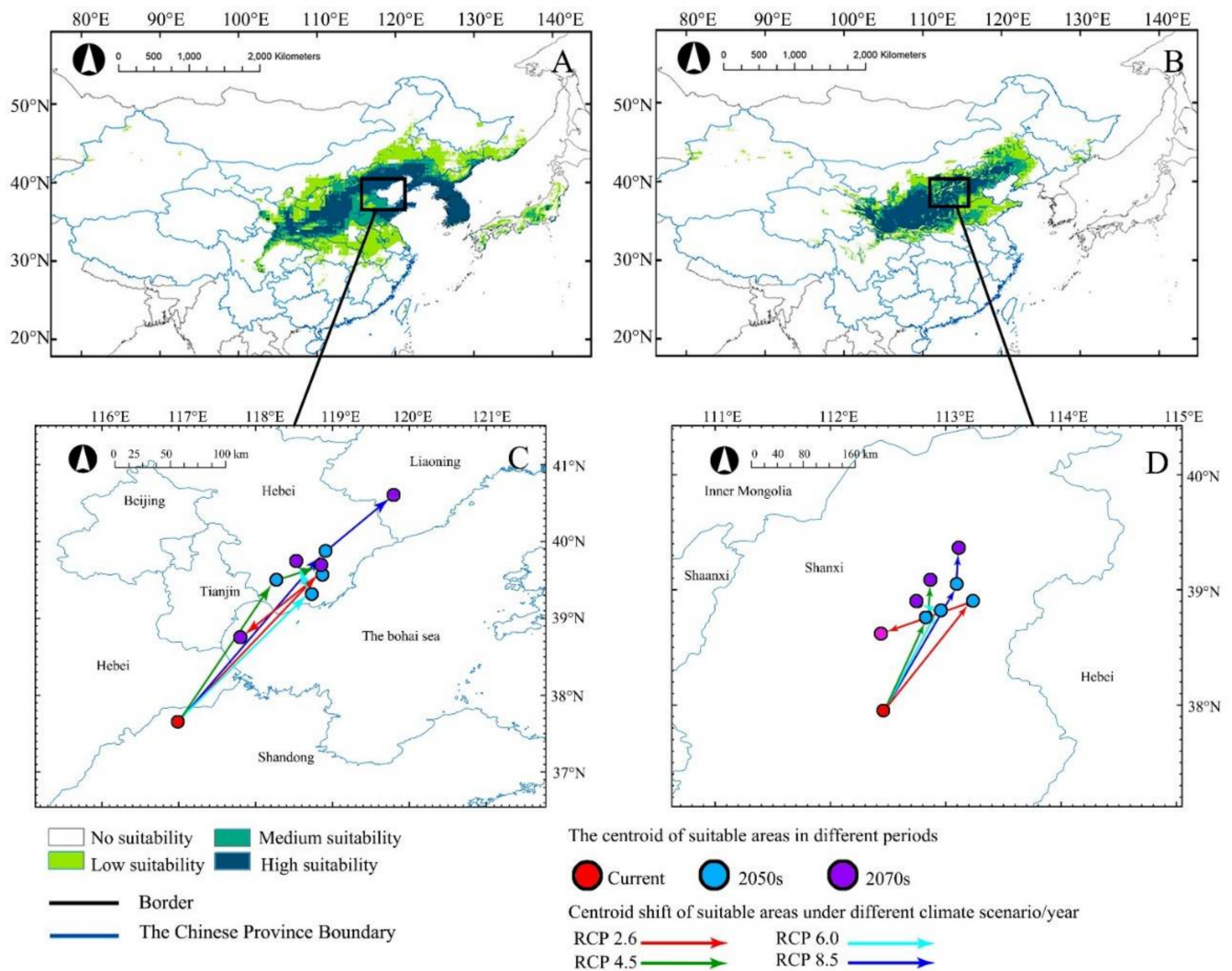


Figure 3. Under different climate scenarios (2050s and 2070s), the current distribution (A,B) and centroid distribution (C,D) of *A. truncatum* (A,C) and *X. sorbifolium* (B,D) are predicted. Arrows indicate the magnitude and direction of the prediction over time.

The potential distribution in current climate of *X. sorbifolium* was mainly in 31°N – 45°N , 101°E – 124°E of China, with a total area of $146.15 \times 10^4 \text{ km}^2$. The suitable habitats of high suitability, medium suitability and low suitability were $37.23 \times 10^4 \text{ km}^2$, $24.29 \times 10^4 \text{ km}^2$ and $35.47 \times 10^4 \text{ km}^2$, respectively (Table 2). The potential suitable habitats of *X. sorbifolium* covered Inner Mongolia Plateau and Loess Plateau (Figure 3).

3.4. Future Potential Suitable Habitats

Compared with the current climate conditions, the potential distribution of *A. truncatum* and *X. sorbifolium* under different climate scenarios have changed in varying degrees.

The model predicted that, under different scenarios, in 2050 and 2070, the potential suitable habitats of *A. truncatum* will increase with the rise in greenhouse gas emission concentration (Table 2). The area of low suitability increased more than that of medium and high suitability. Based on the suitable habitat changes of *A. truncatum*, the potential distribution of *A. truncatum* in the near (2050) and distant (2070) future increased more significantly than that of the current climate, but the reduced potential suitable habitat was, relatively, smaller (Table 3 and Figure 4A1–A8). For example, under RCP 2.6, the total suitable habitat in the 2050s was $115.39 \times 10^4 \text{ km}^2$, and the total suitable habitat in the 2070s was $137.9 \times 10^4 \text{ km}^2$ (Table 2). Compared with the current potential habitat, the gained area

under RCP 2.6—2050 was $45.84 \times 10^4 \text{ km}^2$, with a lost area of only $4.15 \times 10^4 \text{ km}^2$. Under RCP 2.6—2070, the gained area was $27.42 \times 10^4 \text{ km}^2$, with a lost area of only $4.91 \times 10^4 \text{ km}^2$ (Table 3). The suitable habitat at all levels has also increased, and the change of low suitability is the most obvious (Figure 4B1,B2). The area of potential distribution dynamic change of *A. truncatum* under future climate scenarios was shown in Figure 4. The areas of potential distribution gained and lost were approximately similar under different climatic scenarios in the future. The lost area was in the middle and lower reaches of the Yangtze River Plain in China and Japan, and the gained area was in the Northeast Plain of China, the Inner Mongolia Plateau, and Russia. The stable area was distributed in the Loess Plateau and North China Plain (Figure 4B1–B8). The suitable habitat migrated to the northeast with the increase in greenhouse gas emission concentration. Under RCP 8.5—2070, the suitable habitat of *A. truncatum* had the biggest changes, compared to all the other climate scenarios. The area of total suitable habitat was $195.42 \times 10^4 \text{ km}^2$, which was greatly increased compared with the suitable habitat in the current climate. Among the high, medium, and low suitability areas, the area of low suitability increased most obviously. The gained area of suitable habitat under RCP 8.5—2070 was $87.67 \times 10^4 \text{ km}^2$, which was mainly the expansion of low suitable habitat area. The lost area of *A. truncatum* under RCP 8.5—2070 was the largest, which was $7.64 \times 10^4 \text{ km}^2$ (Table 3 and Figure 4A8,B8).

The change pattern of potential distribution was similar between *X. sorbifolium* and *A. truncatum*. With the increase in greenhouse gas emission, the total suitable habitats increased. The area of low suitability increased greatly under future climate scenarios (Table 2). The proportion of increase was also significantly higher than that of loss in suitable habitats (Table 3 and Figure 5A1–A8). The areal dynamics of *X. sorbifolium* in future climate scenarios were shown in Figure 5. Different from *A. truncatum*, the gained area of *X. sorbifolium* was mainly distributed in the Northeast China Plain and Inner Mongolia Plateau. At the same time, suitable habitats also appeared in some western regions of China (Xinjiang and Qinghai of China). The stable area of *X. sorbifolium* was mainly in the Loess Plateau, and the lost area was in the south of the Loess Plateau (Figure 5B1–B8). The area changed the most intensely under RCP 8.5—2070 compared with the other future climate scenarios. The high, medium, and low suitable areas of *X. sorbifolium* took up $58.37 \times 10^4 \text{ km}^2$, $32.34 \times 10^4 \text{ km}^2$, and $102.19 \times 10^4 \text{ km}^2$, respectively (Table 2). The area of low suitability increased significantly, compared with the current distribution of suitable habitats (Table 3 and Figure 5A8,B8). It was inferred that the increase in greenhouse gas emissions had a great impact on the change of both species' suitable habitat.

Table 3. Future suitable habitat changes of *A. truncatum* and *X. sorbifolium*.

	<i>A. truncatum</i> ($\times 10^4 \text{ km}^2$)			<i>X. sorbifolium</i> ($\times 10^4 \text{ km}^2$)		
	Gain	Stable	Loss	Gain	Stable	Loss
RCP2.6—2050	45.84	111.24	4.15	37.56	95.74	1.26
RCP2.6—2070	27.42	110.48	4.91	32.58	94.38	2.63
RCP4.5—2050	44	110.12	5.27	49.49	96.8	0.2
RCP4.5—2070	56.25	110.37	5.02	55.21	96.54	0.46
RCP6.0—2050	39.75	108.51	6.87	41.43	96.13	0.87
RCP6.0—2070	50.37	109.03	6.36	61.45	96.98	0.02
RCP8.5—2050	58.56	109.23	6.16	63.82	96.98	0.03
RCP8.5—2070	87.67	107.75	7.64	95.91	96.99	0.01

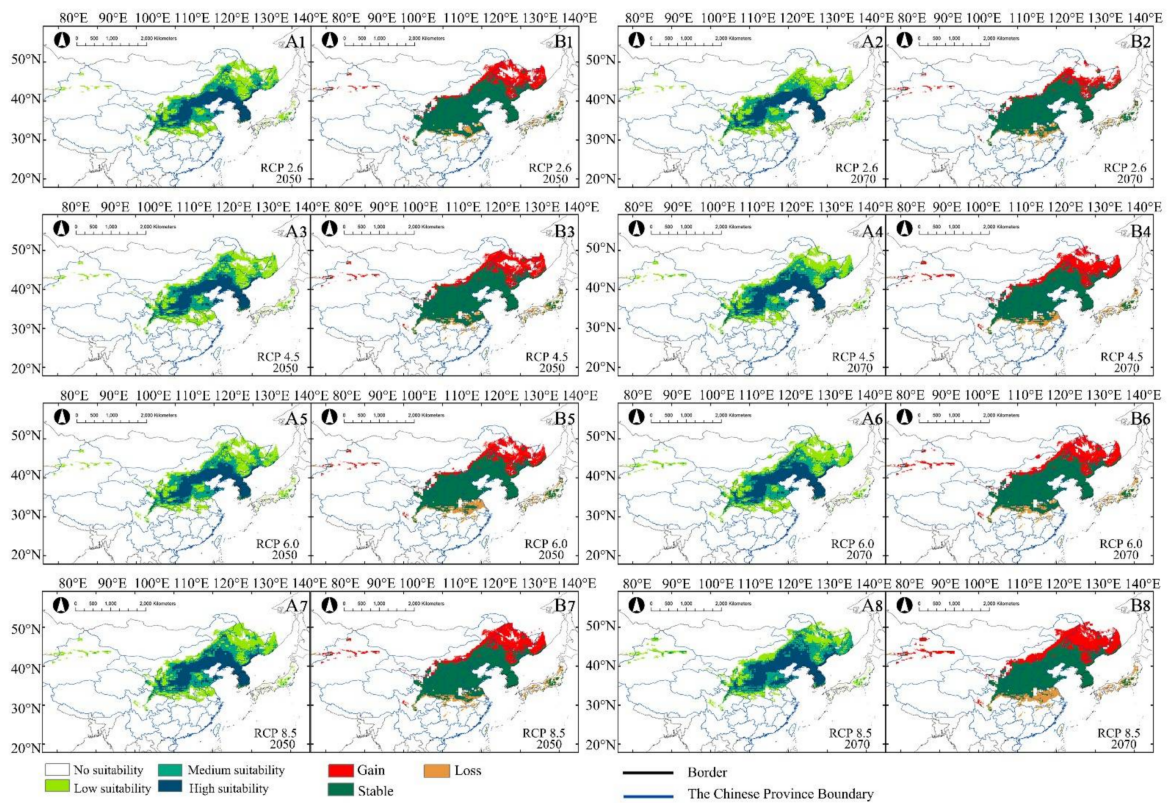


Figure 4. Under future climate change scenarios (2050s and 2070s), (A1–A8) are potentially suitable distributions of *A. truncatum*. (B1–B8) are the area changes of *A. truncatum* compared to the distribution under current climate scenario.

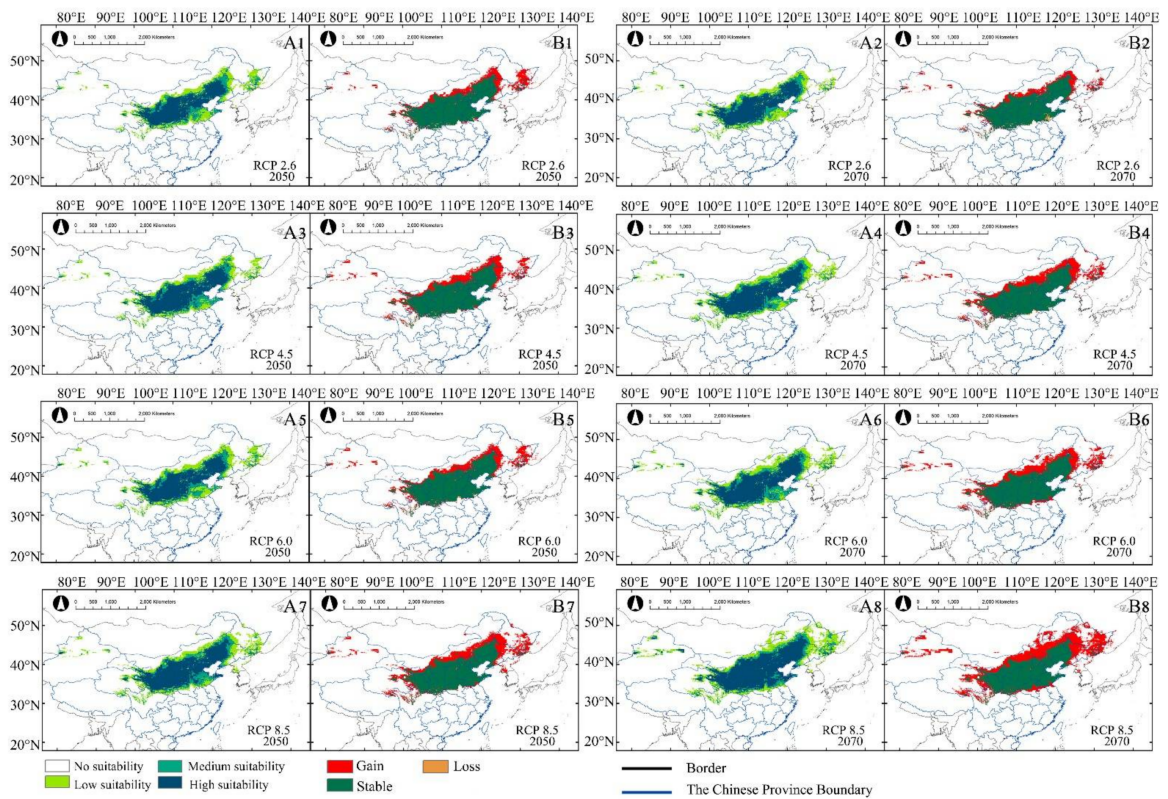


Figure 5. Under future climate change scenarios (2050s and 2070s), (A1–A8) are potentially suitable distributions of *X. sorbifolium*. (B1–B8) are the area changes of *X. sorbifolium* compared to the distribution under current climate scenario.

3.5. Centroid Transition

The MaxEnt model predicted that, with climate change in the future, the potential suitable habitat centroids of *A. truncatum* and *X. sorbifolium* would migrate to the northeast too, and the migration distances would differ under different climate scenarios (Figure 2C,D). Among the four future climate scenarios, the longest centroid migration distances occurred under RCP8.5, with 398.28 and 164.18 km for *A. truncatum* and *X. sorbifolium*, respectively, in the 2070s (Table A1). The centroid migration distances of the two species increased with the greenhouse gas emission concentration, and the effect of greenhouse gas emission on the suitable habitat of *A. truncatum* was greater than that of *X. sorbifolium*.

4. Discussion

The relationship between species potential distribution and environmental variables can be better understood by the response curve given by the MaxEnt model. Generally, when the probability of existence is greater than 0.5, the corresponding environmental variable values are most suitable for plant growth [42]. In this study, the main limiting environmental factors of the two species were also analyzed. It was found that the main limiting environmental factors of *A. truncatum* were mean temperature of driest quarter (-10 to 4 °C), precipitation of wettest month (110 to 680 mm) and the precipitation seasonality (>65). The main limiting environmental factors for the potential distribution of *X. sorbifolium* were mean temperature of driest quarter (-10 to 1 °C), precipitation of wettest month (60 to 150 mm), and precipitation of driest month (1 to 9 mm). The requirements for temperature and precipitation of the two tree species were obviously different. Hence, *X. sorbifolium* is more suitable for planting in arid areas than *A. truncatum*. In addition, the two tree species are significantly affected by monsoon climate: high temperature and rainy in summer, cold and dry in winter [43]. They are suitable for the environment with large seasonal temperature difference. However, the loss of temperature seasonality with the increasing global temperature, driven by climate change, may have a significant negative impact on the photosynthetic activities of these tree species, and other physiological attributes controlled by threshold temperature in study regions [44]. Therefore, the suitable habitats of the two species will also change differently in future. Meanwhile, it is often observed that the emergence of seedlings requires higher precipitation [45]. Nevertheless, the hydrological profile, site characteristics, and ecological needs of related species determine the relationship between water availability and species distribution [46], which also leads to different suitable habitat distribution of *A. truncatum* and *X. sorbifolium* and different migration routes in the future. Their suitable area both span a wide range of longitude. Although the soil conditions in these areas are quite different, soil factors (soil organic carbon content, soil moisture, and soil pH) are not the main environmental factors limiting their distribution. It indicates that the two species can adapt to various soil conditions.

UVB (280–320 nm) is one of the light signal factors in plant growth and development. It regulates plant morphogenesis, circadian rhythm, growth, and development by regulating the expression of related genes through multiple pathways [47,48]. However, high-intensity UVB can cause a lot of reactive oxygen species in plants, which damages proteins and DNA, induces plant defense systems, and promotes plant tissue to produce secondary metabolites [49,50]. In this study, we found that the seasonal variation of UVB (UV2) had a greater impact on the distribution of the suitable areas of *A. truncatum* than that of *X. sorbifolium*, and further quantitative research about the influence should be carried out.

The potential suitable habitat of *A. truncatum* and *X. sorbifolium* showed high sensitivity in different climate scenarios. A common trend of the changes in the suitable habitat of the two tree species was that, under the circumstance of high concentration of greenhouse gas emissions, the expansion area of the suitable habitat was larger than that of the low concentration of greenhouse gas emissions. The suitable habitat and the centroid transfer distance of both species increase with the greenhouse gas emissions; to be exact, both species will migrate to northeast in different degrees. This is in accordance with the fact that, with the warming of the climate, the suitable habitats of most animals and

plants will migrate to high latitudes [51,52]. We found that heat and hydrology have important impacts on the distribution of both species too. If the variation coefficient of temperature and precipitation is within the tolerable ecological range of *A. truncatum* and *X. sorbifolium*, both species will benefit from climate warming, resulting in an increase in suitable habitat area.

In the future extreme climate, we should respond reasonably according to the prediction results, rationalize afforestation, and provide corresponding development strategies [53]. The growth of economic tree species depends on excellent climatic conditions, which requires appropriate precipitation and temperature conditions. Therefore, we should cultivate them and re-establish habitats on the basis of understanding the appropriate climatic conditions [54,55].

Increasing the biodiversity of ecosystems can increase their resistance to climate change [56]. In some ecologically sensitive areas (loess Plateau, Inner Mongolia Plateau, etc.), combining vegetation restoration with some agricultural production projects and appropriately increasing the planting area of local economic tree species can not only solve the shortage of herbal edible oil and limited cultivated land resources, but also realize ecological sustainable development. Increasing the biodiversity of ecologically sensitive areas while increasing the income of local people. However, when selecting introductions, it is also important to introduce interspecific relationships with native species.

The model predicted that new potential suitable habitats appeared for *A. truncatum* in the Northeast Plain, Inner Mongolia Plateau, and Russia, and for *X. sorbifolium*, in the Northeast Plain and Inner Mongolia Plateau, under different climate scenarios. At the same time, the habitats of both species disappeared in some areas. Greenhouse gas emissions changed their habitats. The research can provide valuable information and meaningful maps for the future development of the two economic tree species, which is more conducive to determine the possible but undetermined alternative habitats. According to the prediction results, the suitable area for reintroduction and the priority area for large-scale planting can also be established.

The suitable area predicted by the MaxEnt model does not represent all areas that species can naturally reach in the future. The expansion of distribution area of both species would depend on many factors affecting migration and landscape barriers [27]. We selected several bioclimatic variables that may affect the habitat of both species and established the study regions of both species to speculate its suitable habitat. This cannot be regarded as a completely objective modeling method. Future research needs to explore the environmental stress and related physiological response mechanisms of both species in detail. However, according to the existing information of biological environment variables, some authors have comprehensively pointed out the importance of giving priority to the prediction of an SDM model, including animal and plant protection, species invasion, and pest control [27,57,58]. The model represents a speculation of possibility, which is, indeed, not realistic. However, for the future, we can only speculate based on existing knowledge to provide direction for the future. As our research shows, climate change affects the distribution range of *A. truncatum* and *X. sorbifolium*. In the absence of relevant information, such as limited investigation opportunities and insufficient financial support, ready-made and applicable SDMs may be one of the best tools to deeply understand the potential distribution of species under climate change. This work can provide a reference for the rational and economic afforestation and ecological industry construction of *A. truncatum* and *X. sorbifolium*.

5. Conclusions

Based on 31 environmental factors, the current and future potential distribution areas of *A. truncatum* and *X. sorbifolium* were predicted by a MaxEnt model. The results showed that *A. truncatum* and *X. sorbifolium* were mainly sensitive to environmental variables related to temperature and precipitation. Compared with *X. sorbifolium*, *A. truncatum* was more suitable for warm and humid climates. Under different climate scenarios, the

potential distribution of *A. truncatum* and *X. sorbifolium* migrated northeast to higher latitudes. The change in potential distribution under a high greenhouse emission scenario was greater than that under a low greenhouse emission scenario. The migration scale of suitable habitat of *A. truncatum* was greater than that of *X. sorbifolium*, indicating that *A. truncatum* was more adaptable to climate change.

Author Contributions: Conceptualization, X.Z. and L.W.; methodology, Y.W.; software, Y.W. and Y.Y.; validation, X.Z. and L.W.; formal analysis, C.L. and Y.H.; resources, Y.Y.; data curation, Y.W. and Y.Y.; writing original draft preparation, Y.W.; writing—review and editing, Y.W., Y.Y., and C.L.; visualization, Y.W.; supervision, X.Z.; project administration, S.Y.; funding acquisition, S.Y. All authors have read and agreed to the published version of the manuscript.

Funding: This research was funded by the Central Finance Forestry Science and Technology Promotion and Demonstration Project: Breeding and intensive cultivation demonstration of *Xanthoceras sorbifolium* (Grant Number (2020) 03).

Data Availability Statement: The data presented in this study are available on request from the corresponding author.

Acknowledgments: The authors thank Jihua Zhou, from Key Laboratory of Plant Resources/Beijing Botanical Garden, Institute of Botany, Chinese Academy of Sciences, for his comments and assistance on the manuscript.

Conflicts of Interest: The authors declare that they have no competing interest.

Appendix A

Table A1. The centroid coordinates and centroid migration distance of *A. truncatum* and *X. sorbifolium* under current and future climate scenarios.

	<i>A. truncatum</i> (km)			<i>X. sorbifolium</i> (km)		
	Current	2050s	2070s	Current	2050s	2070s
RCP2.6	117.012° E, 37.671° N	118.003° E, 39.593° N	117.819° E, 38.786° N	112.441° E, 37.942° N	113.208° E, 38.872° N	112.464° E, 38.642° N
RCP4.5	117.012° E, 37.671° N	118.243° E, 39.455° N	118.805° E, 39.702° N	112.441° E, 37.942° N	112.890° E, 38.805° N	112.857° E, 39.047° N
RCP6.0	117.012° E, 37.671° N	118.622° E, 39.362° N	118.575° E, 39.675° N	112.441° E, 37.942° N	112.919° E, 38.805° N	112.808° E, 38.849° N
RCP8.5	117.012° E, 37.671° N	118.820° E, 39.825° N	119.721° E, 40.572° N	112.441° E, 37.942° N	113.091° E, 39.020° N	113.096° E, 39.327° N
	Current to 2050s	2050s to 2070s	Current to 2070s	Current to2050s	2050s to 2070s	Current to 2070s
RCP2.6	230.4	91.12	142.62	123.13	69.4	77.86
RCP4.5	225.4	55.45	274.25	103.64	27.06	128.09
RCP6.0	234.46	35.04	260.88	104.62	10.79	105.8
RCP8.5	286.25	112.94	398.28	132.55	34.14	164.18

References

- Berthel, N.; Schworer, C.; Tinner, W. Impact of Holocene climate changes on alpine and treeline vegetation at Sanetsch Pass, Bernese Alps, Switzerland. *Rev. Palaeobot. Palynol.* **2012**, *174*, 91–100. [[CrossRef](#)]
- Pounds, J.A.; Bustamante, M.R.; Coloma, L.A.; Consuegra, J.A.; Fogden, M.P.L.; Foster, P.N.; La Marca, E.; Masters, K.L.; Merino-Viteri, A.; Puschendorf, R.; et al. Widespread amphibian extinctions from epidemic disease driven by global warming. *Nature* **2006**, *439*, 161–167. [[CrossRef](#)] [[PubMed](#)]
- Qin, H.; Dong, G.; Zhang, Y.B.; Zhang, F.; Wang, M.B. Patterns of species and phylogenetic diversity of *Pinus tabuliformis* forests in the eastern Loess Plateau, China. *For. Ecol. Manag.* **2017**, *394*, 42–51. [[CrossRef](#)]
- Fitzpatrick, M.C.; Gove, A.D.; Sanders, N.J.; Dunn, R.R. Climate change, plant migration, and range collapse in a global biodiversity hotspot: The *Banksia* (Proteaceae) of Western Australia. *Glob. Chang. Biol.* **2008**, *14*, 1337–1352. [[CrossRef](#)]
- Lawler, J.J.; Shafer, S.L.; White, D.; Kareiva, P.; Maurer, E.P.; Blaustein, A.R.; Bartlein, P.J. Projected climate-induced faunal change in the Western Hemisphere. *Ecology* **2009**, *90*, 588–597. [[CrossRef](#)] [[PubMed](#)]

6. Thuiller, W.; Lavorel, S.; Araujo, M.B.; Sykes, M.T.; Prentice, I.C. Climate change threats to plant diversity in Europe. *Proc. Natl. Acad. Sci. USA* **2005**, *102*, 8245–8250. [[CrossRef](#)] [[PubMed](#)]
7. Masson-Delmotte, V.; Zhai, P.; Pirani, A.; Connors, S.L.; Péan, C.; Berger, S.; Caud, N.; Chen, Y.; Goldfarb, L.; Gomis, M.I.; et al. IPCC, 2021: Summary for Policymakers. In *Climate Change 2021: The Physical Science Basis. Contribution of Working Group I to the Sixth Assessment Report of the Intergovernmental Panel on Climate Change*; Cambridge University Press: Cambridge, UK, 2021.
8. Pachauri, R.K.J.S. Climate Change 2007: Synthesis Report. *Contribution of Working Groups I, II and III to the Fourth Assessment Speculum* **2007**, *77*, 586–588. [[CrossRef](#)]
9. Livingston, J.E.; Lövbrand, E.; Alkan Olsson, J. From climates multiple to climate singular: Maintaining policy-relevance in the IPCC synthesis report. *Environ. Sci. Policy* **2018**, *90*, 83–90. [[CrossRef](#)]
10. Wu, L.; Zhang, X.; Jia, Y.; Li, Z.; Fan, Z. Oil Extraction and Physicochemical Properties of Acer Truncatum Bunge Seed with High Oil Content. *J. Chin. Cereals Oils Assoc.* **2020**, *35*, 66–70. [[CrossRef](#)]
11. Wu, Y.; Yuan, W.Q.; Han, X.; Hu, J.Z.; Yin, L.Q.; Lv, Z.L. Integrated analysis of fatty acid, sterol and tocopherol components of seed oils obtained from four varieties of industrial and environmental protection crops. *Ind. Crop. Prod.* **2020**, *154*, 9. [[CrossRef](#)]
12. Kris-Etherton, P.M.; Pearson, T.A.; Wan, Y.; Hargrove, R.L.; Moriarty, K.; Fishell, V.; Etherton, T.D. High-monounsaturated fatty acid diets lower both plasma cholesterol and triacylglycerol concentrations. *Am. J. Clin. Nutr.* **1999**, *70*, 1009–1015. [[CrossRef](#)] [[PubMed](#)]
13. Kinsella, J.E.; Lokesh, B.; Stone, R.A. Dietary n-3 polyunsaturated fatty acids and amelioration of cardiovascular disease: Possible mechanisms. *Am. J. Clin. Nutr.* **1990**, *52*, 1–28. [[CrossRef](#)]
14. Średnicka-Tober, D.; Barański, M.; Seal, C.J.; Sanderson, R.; Benbrook, C.; Steinshamn, H.; Gromadzka-Ostrowska, J.; Rembińska, E.; Skwarło-Sońta, K.; Eyre, M.; et al. Higher PUFA and n-3 PUFA, conjugated linoleic acid, α -tocopherol and iron, but lower iodine and selenium concentrations in organic milk: A systematic literature review and meta- and redundancy analyses. *Br. J. Nutr.* **2016**, *115*, 1043–1060. [[CrossRef](#)]
15. Zhang, T.; Wang, T.; Liu, R.J.; Chang, M.; Jin, Q.Z.; Wang, X.G. Chemical characterization of fourteen kinds of novel edible oils: A comparative study using chemometrics. *LWT-Food Sci. Technol.* **2020**, *118*, 9. [[CrossRef](#)]
16. Zhang, Z.; Zhang, Y.; Ao, Y.; Saunders, M.R.; Wang, X. Diversity of seed and seed oil physicochemical traits of Xanthoceras sorbifolium Bunge. *J. Food Compos. Anal.* **2021**, *96*, 6. [[CrossRef](#)]
17. Xu, C.Q.; Liu, H.; Zhou, S.S.; Zhang, D.X.; Zhao, W.; Wang, S.H.; Chen, F.; Sun, Y.Q.; Nie, S.; Jia, K.H.; et al. Genome sequence of Malaria oleifera, a tree with great value for nervonic acid production. *Gigascience* **2019**, *8*, giy164. [[CrossRef](#)] [[PubMed](#)]
18. Guo, X.; Wang, R.Q.; Chang, R.Y.; Liang, X.Q.; Wang, C.D.; Luo, Y.J.; Yuan, Y.F.; Guo, W.H. Effects of nitrogen addition on growth and photosynthetic characteristics of Acer truncatum seedlings. *Dendrobiology* **2014**, *72*, 151–161. [[CrossRef](#)]
19. Wang, R.K.; Liu, P.; Fan, J.S.; Li, L.L. Comparative transcriptome analysis two genotypes of Acer truncatum Bunge seeds reveals candidate genes that influences seed VLCFAs accumulation. *Sci. Rep.* **2018**, *8*, 15504. [[CrossRef](#)] [[PubMed](#)]
20. Zhang, Y.; Ao, Y.; Liu, J.; Zhao, L.; Zhang, Y. Differences in growth characters of Xanthoceras sorbifolium from different distribution areas and analysis on its correlation with geographical-climatic factors. *J. Plant Res. Environ.* **2019**, *28*, 44–50, 57. [[CrossRef](#)]
21. Zhang, L.; Liu, S.; Sun, P.; Wang, T.; Wang, G.; Zhang, X.; Wang, L. Consensus Forecasting of Species Distributions: The Effects of Niche Model Performance and Niche Properties. *PLoS ONE* **2015**, *10*, e0120056. [[CrossRef](#)] [[PubMed](#)]
22. Guo, Y.; Li, X.; Zhao, Z.; Nawaz, Z. Predicting the impacts of climate change, soils and vegetation types on the geographic distribution of Polyporus umbellatus in China. *Sci. Total Environ.* **2019**, *648*, 1–11. [[CrossRef](#)] [[PubMed](#)]
23. Stoeckli, S.; Felber, R.; Haye, T. Current distribution and voltinism of the brown marmorated stink bug, Halyomorpha halys, in Switzerland and its response to climate change using a high-resolution CLIMEX model. *Int. J. Biometeorol.* **2020**, *64*, 2019–2032. [[CrossRef](#)]
24. Norallahi, M.; Kaboli, H.S. Urban flood hazard mapping using machine learning models: GARP, RF, MaxEnt and NB. *Nat. Hazards* **2021**, *106*, 119–137. [[CrossRef](#)]
25. Carpenter, G.; Gillison, A.N.; Winter, J. Domain-a flexible modeling procedure for mapping potential distributions of plants and animals. *Biodivers. Conserv.* **1993**, *2*, 667–680. [[CrossRef](#)]
26. Xu, W.; Jin, J.W.; Cheng, J.M. Predicting the Potential Geographic Distribution and Habitat Suitability of Two Economic Forest Trees on the Loess Plateau, China. *Forests* **2021**, *12*, 747. [[CrossRef](#)]
27. Chen, Q.H.; Yin, Y.J.; Zhao, R.; Yang, Y.; da Silva, J.A.T.; Yu, X.N. Incorporating Local Adaptation Into Species Distribution Modeling of Paeonia mairei, an Endemic Plant to China. *Front. Plant Sci.* **2020**, *10*, 15. [[CrossRef](#)]
28. Hu, W. Mapping the potential of mangrove forest restoration based on species distribution models: A case study in China. *Sci. Total Environ.* **2020**, *748*, 142321. [[CrossRef](#)]
29. Jhala, H.Y.; Qureshi, Q.; Jhala, Y.V.; Black, S.A. Feasibility of reintroducing grassland megaherbivores, the greater one-horned rhinoceros, and swamp buffalo within their historic global range. *Sci. Rep.* **2021**, *11*, 4469. [[CrossRef](#)]
30. Urvois, T.; Auger-Rozenberg, M.A.; Roques, A.; Rossi, J.P.; Kerdelhue, C. Climate change impact on the potential geographical distribution of two invading Xylosandrus ambrosia beetles. *Sci. Rep.* **2021**, *11*, 1339. [[CrossRef](#)]
31. Wu, C.; Chen, D.; Shen, J.; Sun, X.; Zhang, S. Estimating the distribution and productivity characters of Larix kaempferi in response to climate change. *J. Environ. Manag.* **2021**, *280*, 111633. [[CrossRef](#)]

32. Fick, S.E.; Hijmans, R.J. WorldClim 2: New 1-km spatial resolution climate surfaces for global land areas. *Int. J. Climatol.* **2017**, *37*, 4302–4315. [[CrossRef](#)]
33. New, M.; Hulme, M.; Jones, P. Representing twentieth-century space-time climate variability. Part I: Development of a 1961–90 mean monthly terrestrial climatology. *J. Clim.* **1999**, *12*, 829–856. [[CrossRef](#)]
34. Beckmann, M.; Vaclavik, T.; Manceur, A.M.; Sprtova, L.; von Wehrden, H.; Welk, E.; Cord, A.F. glUV: A global UV-B radiation data set for macroecological studies. *Methods Ecol. Evol.* **2014**, *5*, 372–383. [[CrossRef](#)]
35. Ning, H.; Tang, M.; Chen, H. Impact of Climate Change on Potential Distribution of Chinese White Pine Beetle *Dendroctonus armandi* in China. *Forests* **2021**, *12*, 544. [[CrossRef](#)]
36. Li, J.; Fan, G.; He, Y. Predicting the current and future distribution of three *Coptis* herbs in China under climate change conditions, using the MaxEnt model and chemical analysis. *Sci. Total Environ.* **2020**, *698*, 134141. [[CrossRef](#)]
37. Lobo, J.M.; Jimenez-Valverde, A.; Real, R. AUC: A misleading measure of the performance of predictive distribution models. *Glob. Ecol. Biogeogr.* **2008**, *17*, 145–151. [[CrossRef](#)]
38. Phillips, S.J.; Dudik, M. Modeling of species distributions with Maxent: New extensions and a comprehensive evaluation. *Ecography* **2008**, *31*, 161–175. [[CrossRef](#)]
39. Swets, J.A. Measuring the accuracy of diagnostic systems. *Science* **1988**, *240*, 1285–1293. [[CrossRef](#)] [[PubMed](#)]
40. Shi, X.D.; Yin, Q.; Sang, Z.Y.; Zhu, Z.L.; Jia, Z.K.; Ma, L.Y. Prediction of potentially suitable areas for the introduction of *Magnolia wufengensis* under climate change. *Ecol. Indicators* **2021**, *127*, 14. [[CrossRef](#)]
41. Brown, J.L.; Bennett, J.R.; French, C.M. SDMtoolbox 2.0: The next generation Python-based GIS toolkit for landscape genetic, biogeographic and species distribution model analyses. *PeerJ* **2017**, *5*, 12. [[CrossRef](#)] [[PubMed](#)]
42. Guo, J.; Liu, X.P.; Zhang, Q.; Zhang, D.F.; Xie, C.X.; Liu, X. Prediction for the potential distribution area of *Codonopsis pilosula* at global scale based on Maxent model. *J. Appl. Ecol.* **2017**, *28*, 992–1000. [[CrossRef](#)]
43. Fu, Y.H.; Lu, R.Y.; Guo, D. Projected Increase in Probability of East Asian Heavy Rainy Summer in the 21st Century by CMIP5 Models. *Adv. Atmos. Sci.* **2021**, *38*, 1635–1650. [[CrossRef](#)]
44. Xu, B.; Wang, J.N.; Shi, F.S. Impacts of ontogenetic and altitudinal changes on morphological traits and biomass allocation patterns of *Fritillaria unibracteata*. *J. Mt. Sci.* **2020**, *17*, 83–94. [[CrossRef](#)]
45. Petrie, M.D.; Wildeman, A.M.; Bradford, J.B.; Hubbard, R.M.; Lauenroth, W.K. A review of precipitation and temperature control on seedling emergence and establishment for ponderosa and lodgepole pine forest regeneration. *For. Ecol. Manag.* **2016**, *361*, 328–338. [[CrossRef](#)]
46. Lopez, E.L.; Kerr, S.A.; Sauchyn, D.J.; Vanderwel, M.C. Variation in tree growth sensitivity to moisture across a water-limited forest landscape. *Dendrochronologia* **2019**, *54*, 87–96. [[CrossRef](#)]
47. Raghuvanshi, R.; Sharma, R.K. Response of two cultivars of *Phaseolus vulgaris* L. (French beans) plants exposed to enhanced UV-B radiation under mountain ecosystem. *Environ. Sci. Pollut. Res.* **2016**, *23*, 831–842. [[CrossRef](#)]
48. Romanatti, P.V.; Rocha, G.A.; Veroneze Junior, V.; Santos Filho, P.R.; de Souza, T.C.; Pereira, F.J.; Polo, M. Limitation to photosynthesis in leaves of eggplant under UVB according to anatomical changes and alterations on the antioxidant system. *Sci. Hortic.* **2019**, *249*, 449–454. [[CrossRef](#)]
49. Morales, L.O.; Tegelberg, R.; Brosche, M.; Keinanen, M.; Lindfors, A.; Aphalo, P.J. Effects of solar UV-A and UV-B radiation on gene expression and phenolic accumulation in *Betula pendula* leaves. *Tree Physiol.* **2010**, *30*, 923–934. [[CrossRef](#)] [[PubMed](#)]
50. Qian, S.; Hou, X. Progress of Molecular Mechanisms of Plant UV-B Physiological Effects. *Plant Physiol. J.* **2011**, *47*, 1039–1046. [[CrossRef](#)]
51. Pauli, H.; Gottfried, M.; Dullinger, S.; Abdaladze, O.; Grabherr, G. Recent Plant Diversity Changes on Europe’s Mountain Summits. *Science* **2012**, *336*, 353–355. [[CrossRef](#)]
52. Priti, H.; Aravind, N.A.; Shaanker, R.U.; Ravikanth, G. Modeling impacts of future climate on the distribution of Myristicaceae species in the Western Ghats, India. *Ecol. Eng.* **2016**, *89*, 14–23. [[CrossRef](#)]
53. Pramanik, M.; Paudel, U.; Mondal, B.; Chakraborti, S.; Deb, P. Predicting climate change impacts on the distribution of the threatened *Garcinia indica* in the Western Ghats, India. *Clim. Risk Manag.* **2018**, *19*, 94–105. [[CrossRef](#)]
54. Zimbres, B.Q.C.; Uchoa de Aquino, P.D.P.; Machado, R.B.; Silveira, L.; Jacomo, A.T.A.; Sollmann, R.; Torres, N.M.; Furtado, M.M.; Marinho-Filho, J. Range shifts under climate change and the role of protected areas for armadillos and anteaters. *Biol. Conserv.* **2012**, *152*, 53–61. [[CrossRef](#)]
55. Pramanik, M.; Diwakar, A.K.; Dash, P.; Szabo, S.; Pal, I. Conservation planning of cash crops species (*Garcinia gummi-gutta*) under current and future climate in the Western Ghats, India. *Environ. Dev. Sustain.* **2021**, *23*, 5345–5370. [[CrossRef](#)]
56. Isbell, F.; Craven, D.; Connolly, J.; Loreau, M.; Schmid, B.; Beierkuhnlein, C.; Bezemer, T.M.; Bonin, C.; Bruelheide, H.; de Luca, E.; et al. Biodiversity increases the resistance of ecosystem productivity to climate extremes. *Nature* **2015**, *526*, 574–577. [[CrossRef](#)] [[PubMed](#)]
57. Akhter, S.; McDonald, M.A.; Marriott, R. *Mangifera sylvatica* (Wild Mango): A new cocoa butter alternative. *Sci. Rep.* **2016**, *6*, 32050. [[CrossRef](#)]
58. Ahmadipari, M.; Yavari, A.; Ghobadi, M. Ecological monitoring and assessment of habitat suitability for brown bear species in the Oshtorankooch protected area, Iran. *Ecol. Indicators* **2021**, *126*, 107606. [[CrossRef](#)]